876. LED heat sink and graphite heat sink process technology development with vibration cooling fluid characteristics

Shie-Chen Yang[1], Tsuo-Fei Mao[2], Tzer-Ming Jeng[3], Sheng-Chung Tzeng[4], Tzung-Ying Shie[5], Chih-Liang Chen[6], Po-Tsun Chen[7]
Department of Mechanical Engineering, Chienkuo Technology University
Changhua, 500, Taiwan, R. O. C.
E-mail: [1]*scyang@ctu.edu.tw*, [2]*tfmau@ctu.edu.tw*, [3]*tmjeng@cc.ctu.edu.tw*, [4]*tsc@ctu.edu.tw*,
[5]*evildeat0601@gmail.com*, [6]*a963456789@gmail.com*, [7]*potsun450859@yahoo.com.tw*

Abstract. This study investigated the heat transfer characteristics of LED heat sink and the development process technology of graphite heat sink with micro-sized metal powders. Employing the reverse engineering technology, the three-dimension LED heat sink entity was rebuilt and the heat transfer characteristics of LED heat sink were analyzed by CFD numerical simulation and experimental measurement. The numerical results were validated with experimental results and it showed a good agreement. The experimental and simulation results showed that the heat dissipation of LED device could be removed by natural convection effectively. The difference between the maximum temperature and minimum temperature of cooling efficiency was 10 $^{\circ}$C. For the process technology development of LED graphite heat sink, the graphite powder, metal powder and resin were mixed in specific ratios. The vacuum casting, vacuum pressure casting and rapid die technology were used to manufacture LED graphite heat sink. The experimental results showed that the LED graphite heat sinks developed in this study have advantages of low cost, light weight and attractive appearance as compared with the heat sink of aluminum alloy, and the overall heat transfer capacity is still within acceptable range.

Keywords: LED, heat sink, graphite, natural convection.

Introduction

The Light-Emitting Diodes (LED) uses semiconductor material to convert electric energy into light energy. It is characterized by long life, high efficiency and energy saving, green and environmental protection, which is extensively used in display and lighting industrial applications. The lifetime of LED lamp is twice of fluorescence lamp, but its power consumption is only 1/2 of fluorescence lamp, and 1/4~1/6 of incandescent lamp. As the LED is environment-friendly and energy saving, it becomes the main stream of future lighting fixtures. However the electricity-light conversion efficiency of LED is only about 20 %, the rest of 80 % of electric energy is converted into heat energy. Thus, the component temperature is increased, while the luminous efficiency and component lifetime are reduced, even causing permanent light decay [1-2]. The heat sinking design for LED light source is the fundamental condition for maintaining stable lumen value and lifetime of LED. It is very important for maintaining stable light output. An effective heat sink design can remove the chip junction temperature of LED at a certain level to prolong the lifetime of LED [3]. Using heat sink to increase the cooling area is the most familiar and fundamental method in LED heat management technology. The cooling efficiency indexes of heat sink include heat sink temperature, temperature uniformity and weight. In the application of LED heat sinking design, the natural convection in passive heat sinking is the main heat sinking mode. The natural convection realizes heat exchange by convection heat transfer between air and cooling fins. In recent years, many studies use experiments [4-9] and numerical simulation [10-15] to discuss the natural convection heat transfer characteristics of rectangular fin and pin fin heat sinks. Other studies use optical

1500

analysis [16, 17] and heat transfer characteristics [18, 19] to examine the luminous efficiency of high power LED module. Most of these studies focus the LED heat dissipation on the optimization or manufacturing of LED packaging structure, the substrate material development, while there is little attention on the heat dissipation characteristics, thermal-flow behaviors, thermal resistance and heat dissipation mechanism of LED lamps. At present, the LED heat sinks are mostly metal fins, with heavy weight and high price, which should be reduced to gain competitiveness. In this study, the PHILIPS MASTER LED PAR38 MV lamp was used as the reference component to investigate the heat dissipation characteristics of LED heat sink. Moreover, the graphite powders with micro-sized metal powder and resin were mixed in specific ratios to manufacture the LED graphite heat sink in this study.

Research Method

Physical Model. This study used PHILIPS MASTER LED PAR38 MV lamp as reference component, and the material of the heat sink was aluminum. The related material properties are shown in Table 1. The diameter and height of heat sink were 121.4 mm and 55.9 mm.The average thickness of heat sink fins is 2 mm. The reverse engineering technology was used to rebuild the 3D CAD model of LED heat sink entity, as shown in Fig. 1(a). Then, the numerical simulation and experimental measurement were used to examine the heat transfer characteristics of LED heat sink.

Table 1. Properties of air and heat sink

Material	C_p (J/kg/^{o}C)	μ (N/m^{2}s)	k (W/m/^{o}C)	ρ (kg/m^3)
Air	1005.6	1.834×10^{-5}	2.634×10^{-5}	$\rho = P/RT$
Heat sink (aluminum)	832	–	122.2	2700
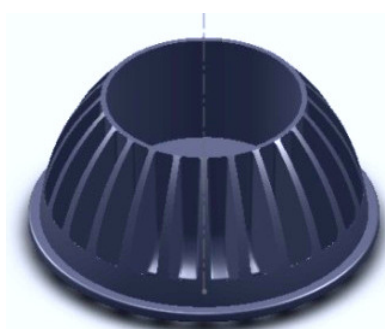
(a) LED heat sink entity model

(b) LED heat sink grids
Fig. 1. Configuration and grid meshes of LED heat sink

Numerical Simulation. In this study, the Ansys Fluent 12.0 and Gambit grid software to simulate the natural convection heat transfer characteristics of LED heat sink. The assumptions of the simulation analysis include: the fluid is steady state, incompressible, neglecting the heat radiation effect and considering the gravity effect. Then the governing equation can be expressed as:

Continuity equation:

$$\frac{\partial u}{\partial x} + \frac{\partial v}{\partial y} + \frac{\partial w}{\partial z} = 0 \tag{1}$$

Momentum equation:

$$u\frac{\partial u}{\partial x} + v\frac{\partial u}{\partial y} + w\frac{\partial u}{\partial z} = -\frac{1}{\rho}\frac{\partial p}{\partial x} + \frac{\mu}{\rho}\left(\frac{\partial^2 u}{\partial x^2} + \frac{\partial^2 u}{\partial y^2} + \frac{\partial^2 u}{\partial z^2}\right) \tag{2}$$

$$u\frac{\partial v}{\partial x} + v\frac{\partial v}{\partial y} + w\frac{\partial v}{\partial z} = -\frac{1}{\rho}\frac{\partial p}{\partial y} + \frac{\mu}{\rho}\left(\frac{\partial^2 v}{\partial x^2} + \frac{\partial^2 v}{\partial y^2} + \frac{\partial^2 v}{\partial z^2}\right) + \rho_a g\beta(T - T_a) \tag{3}$$

$$u\frac{\partial w}{\partial x} + v\frac{\partial w}{\partial y} + w\frac{\partial w}{\partial z} = -\frac{1}{\rho}\frac{\partial p}{\partial z} + \frac{\mu}{\rho}\left(\frac{\partial^2 w}{\partial x^2} + \frac{\partial^2 w}{\partial y^2} + \frac{\partial^2 w}{\partial z^2}\right) \tag{4}$$

Energy equation:

$$\rho_s C_s \frac{\partial T_s}{\partial t} = k_s\left(\frac{\partial^2 T_s}{\partial x^2} + \frac{\partial^2 T_s}{\partial y^2} + \frac{\partial^2 T_s}{\partial z^2}\right) + Q \qquad \text{for solid side} \tag{5}$$

$$u\frac{\partial T}{\partial x} + v\frac{\partial T}{\partial y} + w\frac{\partial T}{\partial z} = \frac{k}{\rho C_p}\left(\frac{\partial^2 T}{\partial x^2} + \frac{\partial^2 T}{\partial y^2} + \frac{\partial^2 T}{\partial z^2}\right) \qquad \text{for fluid side} \tag{6}$$

where ρ is the density, μ is the viscosity coefficient, u, v and w are the velocity components, T is the temperature, P is the pressure, k is the heat transfer coefficient and C_p is the specific heat. The momentum equation y-direction considers the influence of natural convection buoyancy effect, the air density is obtained from the ideal gas equation $\rho = P/RT$, and ρ_a is the reference environmental density value. In numerical simulation, the grid of LED heat sink was built by using Gambit software as shown in Fig. 1(b). The test grid number was from 1,237,854 to 2,453,362 in the simulation. The test result showed when the used grid number is 2,232,564, the average heat sink temperature error value is lower than 0.5 %, and the grid points was chosen for the simulation analysis in this study. In terms of the numerical solver, the finite control volume method with a semi-implicit method for pressure-linked Equations (SIMPLE) algorithm is used to solve the governing equations simultaneously [20]. For improved accuracy, a second-order upwind scheme is applied to the convective terms of the governing equations. The convergence criterion for all dependent variables is a relative error of 10^{-5}.

Experimental Measurement. Fig. 2 shows the experimental systems of LED heat sink. The experimental apparatus consists of a LED heat sink, a data logger, a power supply and a high-resolution temperature measurement camera system. The test section was an aluminum extruded heat sink. First, the thermocouple wires were setup at different measurement positions of the test section, and were connected to the data logger to record the temperature and transmit data to PC for analysis. The measured temperatures were recorded at the steady-state (i.e. temperature change does not exceed 0.2 $^{\circ}$C within 15 minutes). When the steady-state heat balance was reached, the infrared thermal imager was used to photograph the surface temperature distribution of heat sink. As the surface emissivity of aluminum alloy was very

1502

low, its surface was sprayed with water soluble black paint in the experiment, so that the emissivity can be increased to 0.95 to reduce uncertainties of the experiment.
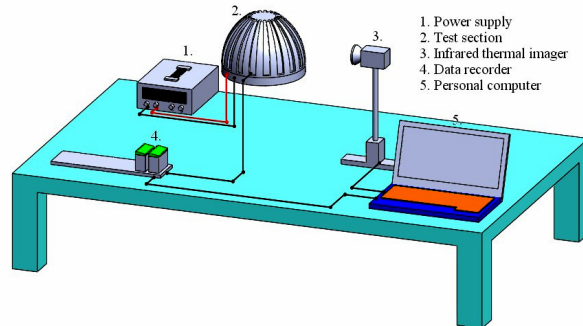

1. Power supply
2. Test section
3. Infrared thermal imager
4. Data recorder
5. Personal computer

Fig. 2. Schematic diagram of experimental system

Development of LED Graphite Heat Sink. The graphite powder, metal powder and resin were mixed in specific ratios to prepare the raw material of LED graphite heat sink. The vacuum casting, vacuum pressure casting and rapid die technology were used to manufacture the LED graphite heat sink. The experimental apparatus are shown in Fig. 3. First, two-liquid resin materials with different composition ratios were poured into the chamber of vacuum casting machine. The samples were made through resin vacuum deaeration, vacuum mixing, vacuum infusion and solidification processes. The samples were used for heat transfer efficiency tests, and then the optimum composition ratio of graphite sample was chosen for the processing of rapid silicone mold. The flowchart of silicone mold processing is shown in Fig. 4.
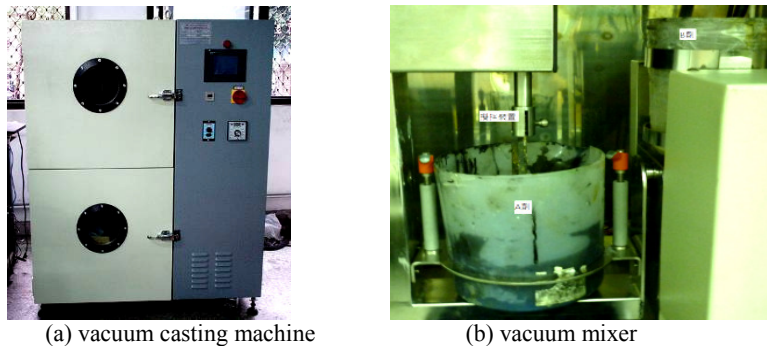

(a) vacuum casting machine　　　　(b) vacuum mixer
Fig. 3. Photos of experimental apparatus to manufacture the LED graphite heat sink
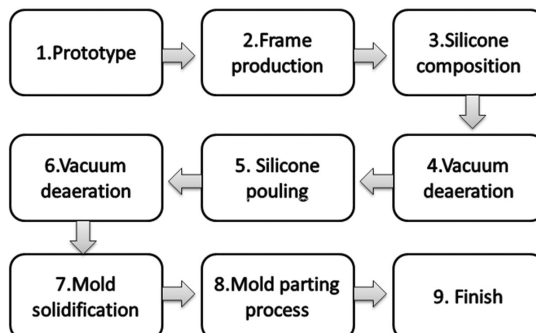

Fig. 4. Flowchart of silicone mold processing

Results and Discussion

Temperature and Fluid Flow Analysis of Aluminum LED Heat Sink. Fig. 5 compares the numerical simulation of temperature distribution of LED heat sink with the infrared thermal image. The required time for the measured temperature to reach a steady state is about 4 h. When the heat dissipation of LED heat sink reaches a steady state, the maximum temperature occurs around the LED heat source chip (51 $^{\circ}$C). There is obvious temperature difference between central and side parts of aluminum heat sink due to the thermal resistances. When the heat sinking is in steady state, the temperature distribution of heat sink is uniform, and the temperature values is between 38 $^{\circ}$C and 40 $^{\circ}$C. Fig. 6 shows the temperature distributions as a function of altitude of LED heat sink. As seen, the temperature variation of heat sink at different heights is lower than 2 $^{\circ}$C, the temperature around the central part of heat sink is about 51 $^{\circ}$C. The heat is dissipated rapidly between heat sink and ambient air by natural convection heat transfer. The maximum temperature of heat sink located at the middle height (y = 30 mm) is about 40 $^{\circ}$C. In addition, according to the graph of relation, the simulation results get agreement with the experimental measuremental result, proving that the numerical simulation can be used to simulate the heat transfer characteristics of LED heat sink accurately. Fig. 7 shows the longitudinal temperature distribution and velocity vector of heat sink in the x-y plane. As shown in Fig. 7(a), the temperatures at the center of LED chip and the bottom of heat sink are 57.8 $^{\circ}$C and 51 $^{\circ}$C, respectively. The temperature difference is about 6.8 $^{\circ}$C. As shown in Fig. 7(b), the vertical flow is in the upward direction due to the difference of density, since air is heated by the sink and becomes lighter than the surrounding air. When the heating air flows upward to a certain height, the effect of buoyancy is reduced, and the air flows downward under gravity and flows into the top gap of heat sink to form two symmetrical vortexes as shown in Fig. 7(b).
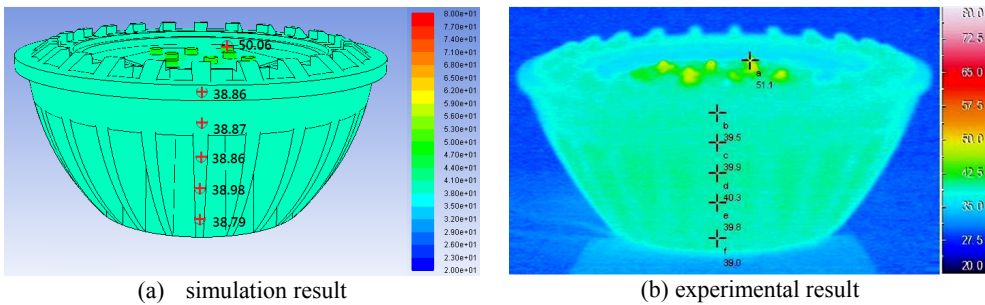
(a)   simulation result   (b) experimental result

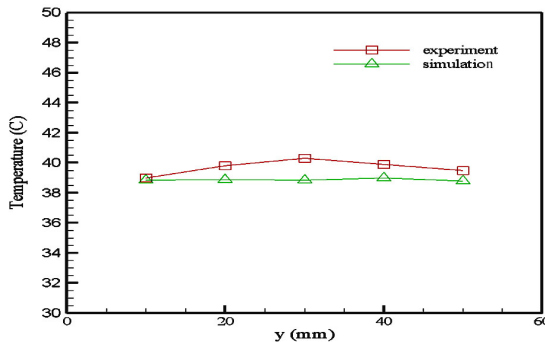**Fig. 5.** Comparison of temperature distributions of LED graphite heat sink

Fig. 6. Temperature distributions as a function of altitude of LED heat sink

Process Design for LED Graphite Cooling Fins. The LED graphite heat sink is characterized by light weight, low cost, high heat conductivity and so on. Table 2 shows the

1504

composition ratios of graphite and micron-sized metal and binding agent. The test pieces were made at six different composition ratios in the experiments. The experimental results showed that when the composition ratio of graphite and micron-sized metal powder is larger, the heat transfer efficiency is better, but the flow ability of the Graphite mixing is worse, and the material cannot even flow in the vacuum casting processing. In order to solve this problem, this study designed a vacuum pressure infusion device, applied 2 kgW/cm^2 pressure in the vacuum process, forcing the mixture of graphite and micron-sized metal resin to fill up the mold cavity. The product of LED graphite heat sink with micron-sized copper powder is shown in Fig. 8.
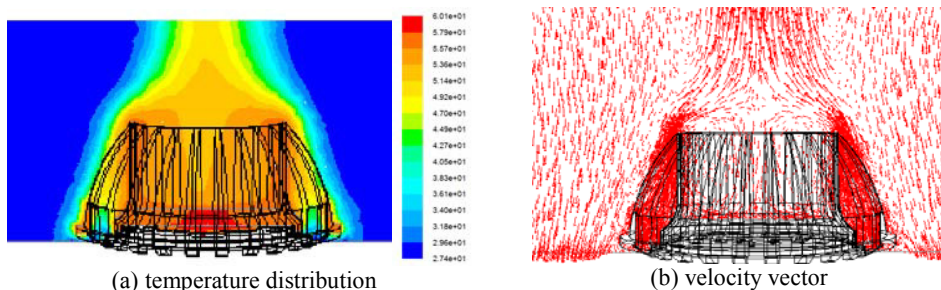
(a) temperature distribution   (b) velocity vector

Fig. 7. Temperature distribution and velocity vector of *x-y* cross section

Table 2. Composition ratio of LED graphite heat sink

	Type	M1 (Al)	M2	M3	M4	M5	M6
Weight percentage (%)	Graphite	0	9.09	16.7	25	17.5	12.5
	Resin	0	90.9	83.3	75	75	75
	Copper powder	0	0	0	0	7.5	12.5

Fig. 8. Product of LED graphite heat sink (Type M2)

Conclusions

This study used numerical simulation and experimental measurement to discuss the heat transfer characteristics of LED heat sink, and designed a light, low cost and high heat conductivity LED graphite heat sink. The following conclusions are derived from experimental results:

(1) The heat transfer characteristics of aluminum alloy cooling fins for LED can be simulated accurately by comparing numerical simulation with experimental measurement.

(2) The LED cooling fins can remove the high heat generated by LED module effectively through natural convection heat transfer.

(3) The LED graphite heat sink is developed successfully in this study. As compared with aluminum alloy heat sink in the same geometric shape, it has advantages of low cost, light weight and attractive appearance.

(4) The theoretical models of heat transfer and mechanical properties can be derived from numerical simulation and heat transfer experiment for LED graphite heat sinks with different constituents in the future.

Acknowledgements

References

[1] **Narendran N., Gu Y.** Life of LED-based white light sources. IEEE/Optic. Soc. Amer. J. Displ. Tech., Vol. 1, 2005, p. 167 – 171.
[2] **Schubert E. F.** Light-Emitting Diodes. Cambridge University Press, New York, 2003.
[3] **Lu D., Wong C. P.** Materials for Advanced Packaging. New York: Springer, 2008, p. 630 – 644.
[4] **Starner K. E., McManus H. N.** An experimental investigation of free convection heat transfer from rectangular fin arrays. ASME J. Heat Transfer, Vol. 85, 1963, p. 273 – 278.
[5] **Welling J. R., Wooldridge C. B.** Free convection heat transfer coefficients from rectangular vertical fins. Trans. ASME J. Heat Transfer, Vol. 87, 1965, p. 439 – 444.
[6] **Harahap F., McManus H. N.** Natural convection heat transfer from horizontal rectangular fin arrays. J. Heat Transfer, Vol. 89, 1967, p. 32 – 38.
[7] **Ledezma G., Bejan A.** Heat sinks with sloped plate fins in natural and forced convection. Int. J. Heat Mass Transfer, Vol. 39, 1996, p. 1773 – 1783.
[8] **Harahap F., Setio D.** Correlations for heat dissipation and natural convection heat-transfer from horizontally-based, vertically-finned arrays. Appl. Energy, Vol. 69, 2001, p. 273 – 278.
[9] **Huang R. T., Sheu W. J., Wang C. C.** Orientation effect on natural convective performance of square pin fin heat sinks. Int. J. Heat Mass Transfer, Vol. 51, 2008, p. 2368 – 2376.
[10] **Baskaya S., Sivrioglu M., Ozek M.** Parametric study of natural convection heat transfer from horizontal rectangular fin arrays. Int. J. Therm. Sci., Vol. 39, 2000, p. 797 – 805.
[11] **Dialameh L., Yaghoubi M., Abouali O.** Natural convection from an array of horizontal rectangular thick fins with short length. Appl. Therm. Eng., Vol. 28, 2008, p. 2371 – 2379.
[12] **Yu S. H., Lee K. S., Yook S. J.** Natural convection around a radial heat sink. Int. J. Heat Mass Transfer, Vol. 53, 2010, p. 2935 – 2938.
[13] **Yu S. H., Lee K. S., Yook S. J.** Optimum design of a radial heat sink under natural convection. Int. J. Heat Mass Transfer, Vol. 54, 2011, p. 2499 – 2505.
[14] **Ren R. B., Yang D. G., Liu D. J.** Structural design and heat dissipation research of integrated 3W white LED miner's lamp. 12th International Conference on Electronic Packaging Technology and High Density Packaging, 2011, p. 1061 – 1065.
[15] **Cheng H. H., Huang D. S., Lin M. T.** Heat dissipation design and analysis of high power LED array using the finite element method. Microelectronics Reliability, Vol. 52, 2012, p. 905 – 911.
[16] **Tran N. T., Shi F. G.** Studies of phosphor concentration and thickness for phosphor-based white light-emitting-diodes. J. Lightwave Tech., Vol. 26, 2008, p. 3556 – 3559.
[17] **Zhou Y., Tran N. T., Lin Y. C., He Y., Shi F. G.** One-component, low-temperature, and fast cure epoxy encapsulant with high refractive index for LED applications. IEEE Trans. Adv. Packag., Vol. 31, 2008, p. 484 – 489.
[18] **Christensen A., Graham S.** Thermal effects in packaging high power light emitting diode arrays. Appl. Thermal Eng., Vol. 29, 2009, p. 364 – 371.
[19] **Yin L., Yang W., Guo Y., Ma K., Li S., Chen M., Li J., Zhang J.** Multi-chip integrated high-power white LED device on the multi-layer ceramic substrate. Proc. IEEE 58th Electron. Compon. Technol. Conf., 2008, p. 790 – 794.
[20] **Patackar S. V., Spalding D. B.** A calculation procedure for heat, mass and momentum transfer in three-dimensional parabolic flows. Int. J. Heat Mass Transfer, Vol. 15, 1972, p. 1787 – 1806.